The N-terminal Ac-EEED sequence plays a role in α-smooth-muscle actin incorporation into stress fibers

Sophie Clément[1],*, Boris Hinz[2],*, Vera Dugina[3], Giulio Gabbiani[1] and Christine Chaponnier[1],‡

[1]Dept of Pathology and Immunology, CMU, Geneva, Switzerland
[2]Laboratory of Cell Biophysics, Ecole polytechnique Fédérale de Lausanne (EPFL), 1015 Lausanne, Switzerland
[3]Moscow State University, 119899 Moscow, Russia
*Both authors contributed equally to this work
‡Author for correspondence (e-mail: christine.chaponnier@medecine.unige.ch)

Summary

We have previously shown that the N-terminal sequence AcEEED of α-smooth-muscle actin causes the loss of α-smooth-muscle actin from stress fibers and a decrease in cell contractility when introduced in myofibroblasts as a cell-penetrating fusion peptide. Here, we have investigated the function of this sequence on stress fiber organization in living cells, using enhanced green fluorescent protein (EGFP)-tagged α-smooth-muscle actin. The fusion peptide provokes the gradual disappearance of EGFP fluorescence of α-smooth-muscle actin from stress fibers and the formation of hitherto unknown rod-like structures. In addition to α-smooth-muscle actin, these structures contain cytoplasmic actins, gelsolin and cofilin but not other major actin-binding proteins. These rod-like structures are also visible in wild-type fibroblasts during normal cell spreading, suggesting that they represent a physiological step in the organization of α-smooth-muscle actin in stress fibers. Fluorescence-recovery-after-photobleaching experiments suggest that the fusion peptide reduces the dynamics of α-smooth-muscle actin and its incorporation in stress fibers. Here, we propose a new mechanism of how α-smooth-muscle actin is incorporated in stress fibers involving the sequence Ac-EEED.

Supplementary material available online at
http://jcs.biologists.org/cgi/content/full/118/7/1395/DC1

Key words: Actin isoforms, GFP fusion protein, Actin dynamism, Cytoskeleton, Actin-binding protein

Introduction

It has become generally accepted that myofibroblasts, specialized contractile fibroblasts displaying smooth-muscle-cell-like features, are responsible for granulation tissue contraction during wound healing and pathological contractures (Serini and Gabbiani, 1999; Powell et al., 1999). Myofibroblasts are defined morphologically and immunohistochemically by the expression and organization of cytoskeletal proteins (Sappino et al., 1990; Schmitt-Graff et al., 1994). α-Smooth-muscle actin (α-SMA), the actin isoform most prominent in vascular smooth-muscle cells (Darby et al., 1990; Skalli et al., 1986), is considered the most reliable marker of myofibroblastic differentiation (Tomasek et al., 2002).

Actin is a major component of the cytoskeleton in all eukaryotic cells and is encoded by a gene family producing highly conserved proteins, including six different isoforms in vertebrates: α-skeletal, α-cardiac, α-smooth-muscle, γ-smooth muscle, β-cytoplasmic and γ-cytoplasmic actin. Iso-actins are expressed in a tissue-specific fashion that is conserved across species (Herman, 1993; Khaitlina, 2001; Rubenstein, 1990). Displaying only small differences in their overall amino acid sequences, actin isoforms have unique N-termini (Vandekerckhove and Weber, 1978) and we have therefore hypothesized that this domain probably represents a candidate for functional specialization mediated through specific binding. Consistent with this hypothesis, previous studies showed that the monoclonal antibody anti-αsm-1, which is directed against α-SMA (Skalli et al., 1986) and recognizes its N-terminal tetrapeptide Ac-EEED as epitope (Chaponnier et al., 1995), induces α-SMA polymerization in vitro (Chaponnier et al., 1995). Microinjection of the peptide Ac-EEED into cultured fibroblasts leads to the disappearance of α-SMA-specific immunodetection (Chaponnier et al., 1995), whereas microinjection of equivalent peptide sequences of other actin isoforms has no effect, suggesting that the peptide interferes with the function of this specific isoform. Moreover, when fused to the Antennapedia third helix sequence (pAntp-Pro50) to allow cell penetration (Derossi et al., 1994), the Ac-EEED fusion peptide (SMA-FP) inhibits contractility of myofibroblasts in vitro and granulation tissue contraction in vivo (Hinz et al., 2002).

To further understand how the N-terminus of α-SMA exerts these activities, we created α-SMA tagged with enhanced green fluorescent protein (EGFP), which allows us to follow the effects of SMA-FP on α-SMA-organization in living cells. We provide evidence that SMA-FP blocks α-SMA-dynamics and its incorporation in stress fibers. One consequence of this
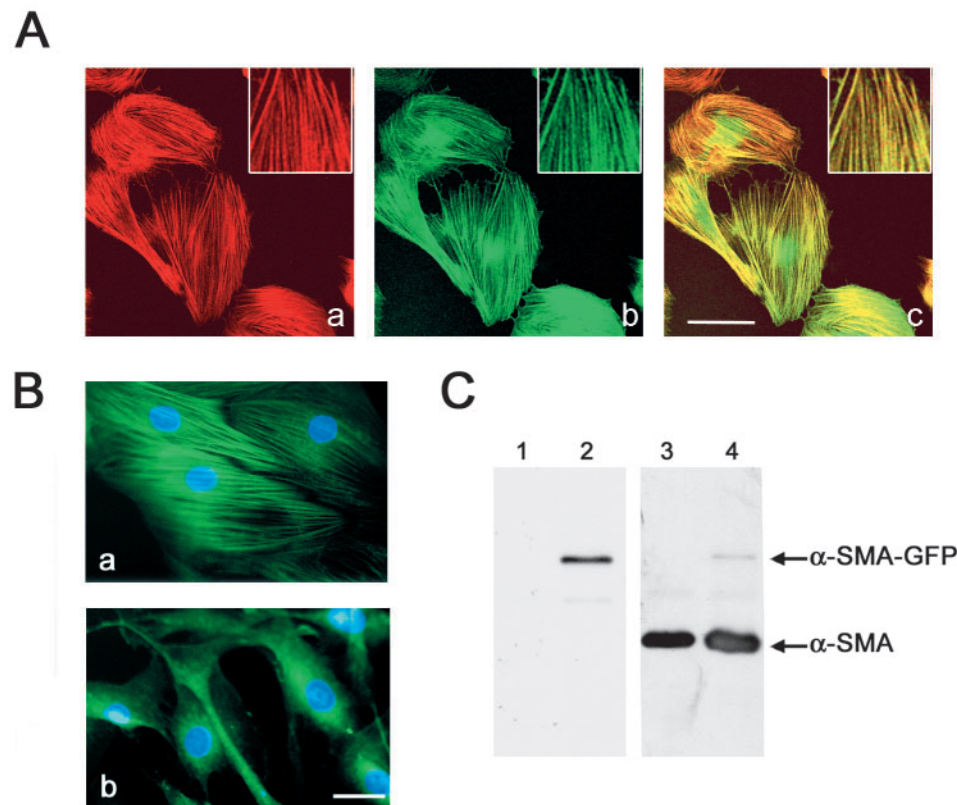
A

B

C

Fig. 1. Characterization of transfected cells. REF-52 cells were transfected with α-SMA-EGFP and cells stably expressing α-SMA-EGFP were obtained after FACS sorting and G418 selection. (A) In the majority of cells, α-SMA-EGFP is incorporated into actin stress fibers (see inset), as indicated by indirect double immunofluorescence of fixed cells. (a) α-SMA was visualized with anti-α-sm1 antibody, (b) α-SMA-EGFP was visualized with anti-GFP antibody. (c) Overlay of a and b. Scale bar, 50 μm. (B) Transfected REF-52 cells were grown for 5 days in culture medium containing either 2% FCS (a) or 20% FCS (b). Cells were fixed and α-SMA-EGFP organization was assessed by fluorescence microscopy. Scale bar, 20 μm. (C) Cell homogenates of non-transfected cells (lanes 1 and 3) and transfected cells (lanes 2 and 4) were analyzed on a 10% SDS-PAGE and immunoblotted with anti-GFP antibody (lanes 1-2) and anti-SMA antibody (lanes 3-4). The anti-GFP antibody detected a single 80 kDa band corresponding to the calculated molecular mass of the fusion protein (42 kDa actin+36 kDa EGFP). This band was also recognized by the anti-α-SMA antibody. Transfected and non-transfected cells both showed the endogenous α-SMA band of 42 kDa.

perturbed incorporation of α-SMA in stress fibers appears to be a dramatic reduction of α-SMA-dependent contractility.

Materials and Methods

α-SMA-EGFP fusion construct

α-SMA cDNA was amplified by PCR using the sequence-specific primers 5′-CTCGAGCTCGAAGCTGCTCCAGCTATGTGTGAA-3′ (sense) and 5′- GCGACCGGTGGCTTTCCAAGTCGGTTCATCTC-3′ (antisense) that contain a Sac1 and an Age1 restriction site, respectively. A plasmid encoding α-SMA tagged with VSVG (Mounier et al., 1997) was used as template for amplification. PCR cycling conditions (30 cycles) consisted of 1 minute denaturation at 94°C, 1 minute annealing at 55°C, and 1 minute extension at 72°C. The resultant α-SMA sequence was inserted into pEGFP-N1 (Clontech, Palo Alto, CA). The sequence of the generated plasmid was checked with T7 and Sp6 primers.

Cell culture and transfection

Rat embryonic fibroblasts (REF-52 cells) were grown in Dulbecco's Modified Eagle's Medium (DMEM; Gibco-BRL, Life Technologies AG, Basel, Switzerland) supplemented with 100 U/ml penicillin, 100 μg/ml streptomycin, 2 mM L-glutamine and 10% fetal calf serum (FCS) (Hyclone, Logan, UT) at 37°C, 5% CO_2. Cells were transfected with the α-SMA-EGFP construct using FuGENE 6 transfection reagent (Roche Diagnostics AG, Rotkreuz, Switzerland) according to the manufacturer's instructions, and, after 48 hours, were selection-pressured for two passages with 2 mg/ml G418 (Calbiochem-Novabiochem Corporation, San Diego, CA). Cells were then collected and sorted into three populations of EGFP-positive cells (high, medium and low expressors) using a FACStar+ flow cytometer (Becton Dickinson, BD Biosciences, Basel, Switzerland). The

population of medium-expressor cells was used for cloning by FACS-sorting single cells into the wells of 96-well plates. Fifteen clones exhibited normal cell morphology and significant incorporation of α-SMA-EGFP into stress fibers. Experiments were generally performed with one clone (SM02), and all results were confirmed with two other clones. Cells were then split and grown either in plastic dishes in DMEM-FCS (10%) for cell expansion or in 1 ml glass chambers (produced by gluing a silicone ring, diameter 25 mm, onto a 22×22 mm coverslip) in DMEM-FCS (2%) to test expression and organization of α-SMA-EGFP (Hinz et al., 2003). Transfected or non-transfected cells were treated with either 5 μg/ml SMA-FP or α-skeletal actin (α-SKA)-FP as a control, produced as previously described (Hinz et al., 2002).

Spreading experiments

For spreading experiments, cells transfected with α-SMA-EGFP were cultured in the presence of 2% FCS for 4 days, trypsinized and seeded in culture dishes with F12 medium (Gibco). Cells were fixed after 4, 6, 8 and 12 hours and were stained with anti-α-SMA and anti-β-cytoplasmic actin antibodies (see below). At each time point, cells displaying rod-like structures (RLSs) or stress fibers were counted under the microscope (n=200 for each condition). In a second experiment, SMA-FP (5 μg/ml) was added 2 hours after spreading for a further 2 hours.

Electrophoretic and immunoblot analysis

For immunoblotting, cells were thoroughly scraped from culture dishes in sample buffer [62.5 mM Tris-HCl, pH 6.8, 2% sodium dodecyl sulfate (SDS), 10% glycerol, 50 mM DTT, 0.01% bromophenol blue]. Total cell lysates were run on 10% SDS-minigels (Bio-Rad Laboratories AG, Glattbrugg, Switzerland) (Laemmli, 1970) and electroblotted to nitrocellulose according to Towbin et al.

Fig. 2. Time-lapse observation of α-SMA-EGFP in SMA-FP-treated cells and determination of the morphological features of RLSs. (A) Cells were trypsinized and plated into observation chambers for 3 days in DMEM-FCS (2%). Before recording, cells were mounted on an inverted confocal microscope (LSM510, Carl Zeiss) and treated with SMA-FP. EGFP images were collected every 2 minutes for 90 minutes. RLSs appeared mainly in the submembrane area or along stress fibers (arrowhead); fluorescence in the α-SMA-EGFP positive stress fibers (arrows) decreases over time. Scale bar, 20 μm. See also videos in supplementary material. (B) Length (a) and diameter (b) of RLSs were determined on digitized confocal images using Openlab 3.0.6 software. Their length varied from 2 to 20 μm and their diameter from 0.1 to 1.2 μm. (C) α-SMA-EGFP transfected cells were either non-treated (Cont), or treated for 60 minutes with control peptide SKA-FP or SMA-FP. Reversibility of SMA-FP treatment was assessed by removing the peptide by washing cells with fresh medium for 60 minutes. The percentage of EGFP-positive cells displaying RLSs was estimated by counting a minimum of 200 cells. RLSs were visible in approximately 60% of the transfected cells and the effect of SMA-FP was reversible. Controls in the absence of SMA-FP or in the presence of SKA-FP were close to baseline. Bars represent s.e.m. (**$P \leq 0.001$ compared to control). (D) Non-transfected cells were treated with 5 μg/ml SMA-FP for 30 minutes, fixed and permeabilized with 1% paraformaldehyde for 10 minutes followed by methanol for 3 minutes and stained with anti-actin antibody (see Table 1). By using this detergent-free procedure, RLSs were also found in non-transfected cells. Scale bar, 20 μm.
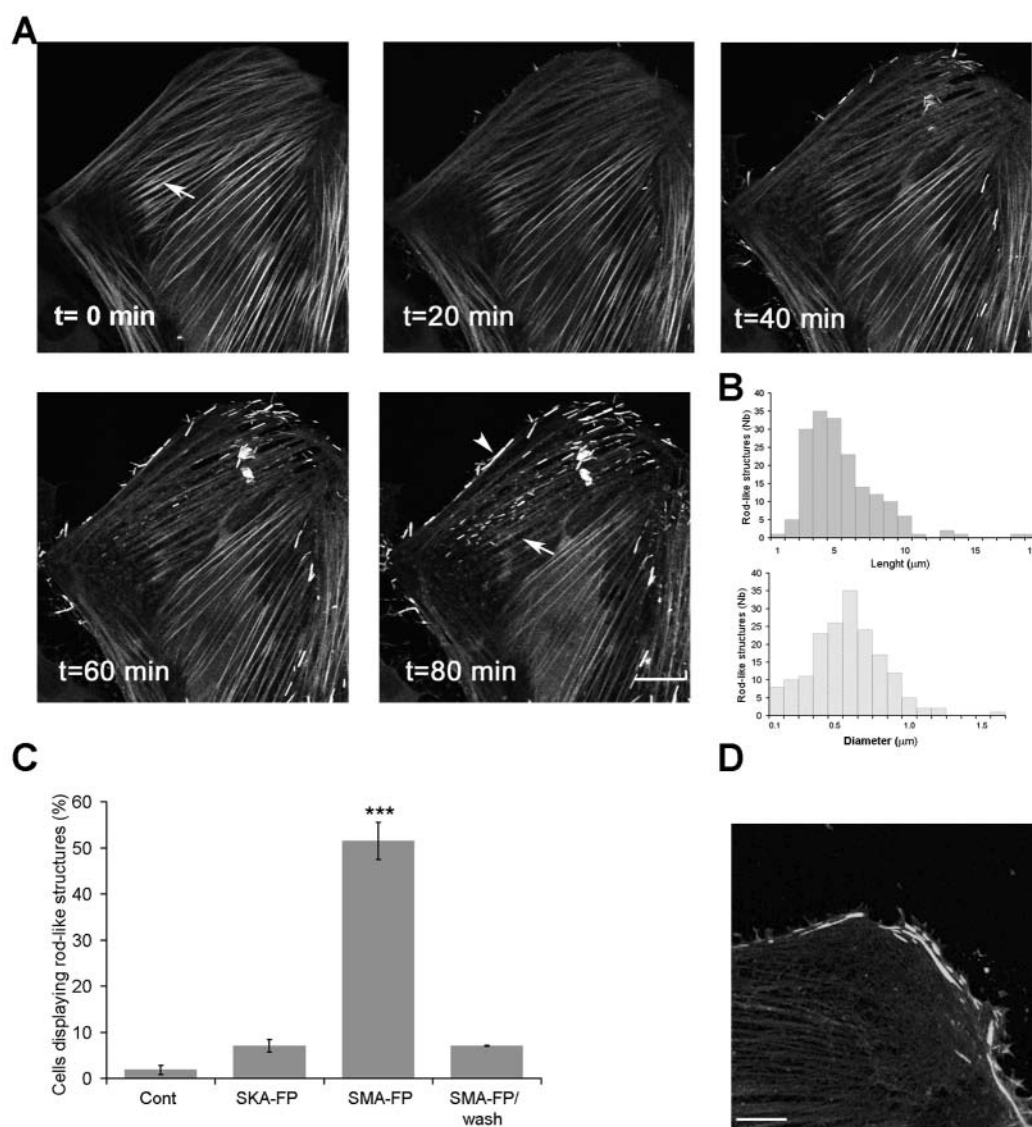
(Towbin et al., 1979). Nitrocellulose membranes were incubated with anti-αsm-1 (Skalli et al., 1986) and anti-GFP (Molecular Probes Inc, Eugene, OR) diluted in Tris-buffered saline (TBS) solution containing 3% BSA and 0.1% Triton X-100 for 2 hours at room temperature. After three washes with TBS, a second incubation was performed with peroxidase-conjugated affinity-purified goat anti-rabbit IgG (Jackson Immunoresearch Laboratories, West Grove, PA) at a dilution of 1:10,000 in TBS containing 0.1% BSA and 0.1% Triton X-100. Peroxidase activity was developed using the ECL western blotting system (Amersham, Rahn AG, Zürich, Switzerland), according to the manufacturer's instructions followed by scanning of the blots (Arcus II; Agfa, Mortsel, Belgium).

Immunofluorescence microscopy

For immunofluorescence staining, cells were fixed in 1% paraformaldehyde in phosphate-buffered saline solution (PBS) for 10 minutes at RT, followed by three washes with PBS and 3 minutes treatment with methanol at –20°C. Subsequently, cells were stained with a large panel of primary antibodies (Table 1). Samples were then incubated with either Alexa Fluor® 568-conjugated anti-mouse or anti-rabbit Ig (Molecular Probes, diluted 1:500 in PBS), for 30 minutes at RT. F-actin was probed with Alexa Fluor® 568 phalloidin (Molecular Probes) on cells fixed only with 1% paraformaldehyde. After washing in PBS, cells were mounted in polyvinyl alcohol (PVA) (Lennette, 1978): 50 mM Tris-phosphate pH 9.0, 0.1% chlorobutanol, 20% polyvinyl alcohol, 0.5‰ phenol red, 20% glycerol. Images were taken with either a Zeiss Axiophot microscope (Carl Zeiss, Oberkochen, Germany; using an 63× oil immersion objective) equipped with a high-sensibility color camera (Axiocam, Zeiss) or a confocal microscope (LSM510, Zeiss) with similar optics at 3× zoom, and printed with a digital Fujifilm Pictography 4000 printer (Fujifilm, Tokyo, Japan).

Live time-lapse observations and fluorescence recovery after photobleaching (FRAP) analyses

For video-microscopy, cells were grown in observation chambers (see above) for 3 days in DMEM-FCS (2%). Prior to recording, medium was changed to serum-free F12 and cells were mounted on LSM510 confocal microscope equipped with a Plan-Neofluar 63× 1.3 Ph3 objective and maintained at 37°C with a heating stage and CO_2-incubation chamber. GFP images were acquired every 2 minutes at 488 nm excitation and 515-545 nm emission over a period of time of 90 minutes from cells treated with either SMA-FP or SKA-FP as a control. For spreading experiments, SM02 cells were seeded in observation chambers in F12 medium supplemented with 2% FCS and allowed to spread for 2 hours. Cell-spreading was imaged on an Axiovert 200M equipped with an array laser confocal spinning wheel (Nipkow disc; Visitech, Sunderland, UK) using a 63×, 1.4 NA oil-immersion objective (Carl Zeiss). Images were acquired every 10 minutes for 15 hours by using a cooled, 16-bit CCD camera (CoolSnap HQ; Roper Scientific, Trenton, NJ) operated by Metamorph 6.1 software (Universal Imaging, West Chester, PA).

In FRAP experiments, bar and square-shaped regions or complete RLSs were bleached with 100% transmission (λ=488 nm) with 10 iterations each lasting 1 second, and recovery was monitored at 1 minute intervals in control conditions or on cells treated for 15 minutes with FP before photobleaching. To quantify FRAP, length and grayscale pixel-values were measured on digitized confocal images using the Openlab 3.0.6 software (Improvision, Basel, Switzerland). The average rate of movement was determined by calculating distance versus time. Mean values were calculated from at least ten cells from three independent experiments per condition.

Statistical analysis

Quantitative results are presented as mean values±s.e.m. Differences between mean values were calculated by using the Student's t test and were considered to be statistically significant at values of $P \leq 0.001$(***).

Results

Characterization of α-SMA-EGFP

After FACS sorting and G418 selection, we obtained 15 clones that stably expressed α-SMA-EGFP at different expression levels in stress fibers. Clones showed normal cell morphology and proliferation rates compared with wild-type REF-52 cells. Moreover, expression of exogenous α-SMA-EGFP did not interfere with endogenous α-SMA expression when induced by TGFβ and low serum levels (data not shown). For this study we used one clone (SM02) that, in approximately 80% of the cells, resulted in cells which had α-SMA-EGFP organized in stress fibers, colocalizing perfectly with endogenous α-SMA (Fig. 1A). Like endogenous α-SMA, incorporation of α-SMA-EGFP in stress fibers was induced by 2% FCS in the culture medium (Fig. 1B, a) and by TGFβ (data not shown). Thus, the organization of α-SMA-EGFP was regulated by TGFβ, as previously described for endogenous α-SMA (Moustakas and Stournaras, 1999) (data not shown) and expression of α-SMA-EGFP did not appear to interfere with cell function.

To ensure that the expression of α-SMA-EGFP did not alter the dynamic properties of α-SMA, we cultured SM02 cells in different concentrations of FCS, ranging from 2% to 20% FCS. In 20% FCS, cells did not exhibit α-SMA-EGFP-positive stress fibers (Fig. 1B, b) as previously observed for endogenous α-SMA in REF-52 cells (Hinz et al., 2003). Expression of α-SMA-EGFP was also tested

Table 1. Molecular characteristics of rod-like structures

Molecular component		Presence in RLS	Antibody used (provenance/company)
Actin isoforms	Total actin	+	Mouse mAb (clone Ac40, Sigma, St Louis, MO)
	α-SMA	+	Mouse mAb [α-sm-1, (Skalli et al., 1986)]
	β-Cyto actin	+	Mouse mAb developed in the laboratory
	γ-Cyto actin	+	Mouse mAb developed in our laboratory (manuscript in preparation)
Actin binding proteins	Gelsolin	+	Rabbit polyclonal (Chaponnier and Gabbiani, 1989)
	Cofilin	+	Rabbit polyclonal [gift from Pekka Lappalainen, University of Helsinki, Finland, (Rodal et al., 1999)]
	Calponin	–	Mouse mAb (Sigma)
	Tropomyosin	–	Rabbit polyclonal [gift from Peter Gunning, The Children's Hospital Westmead, Australia; (Percival et al., 2000)]
	Palladin	–	Rabbit polyclonal (gift from Olli Carpèn, University of Helsinki, Finland)
	SM22	–	Mouse mAb (clone 1B8, gift from Saverio Sartore, university of Padua, Italy)
	caldesmon	–	Rabbit polyclonal [gift from Gabriele Pfitzer, University of Cologne, Germany; (Pfitzer et al., 2001)]
	α-Actinin	–	Mouse mAb (clone BM-75.2, Sigma)
	MHC from aorta	–	Rabbit polyclonal (Benzonana et al., 1988)
	MHC from platelets	–	Rabbit polyclonal (Benzonana et al., 1988)
	MLC	–	Rabbit polyclonal (Santa Cruz Biotech, Santa Cruz, CA)
	Arp2/3	–	Rabbit polyclonal (Svitkina et al., 2003)
Focal adhesion proteins	Vinculin	–	Mouse mAb (clone hVin-1, Sigma)
	Talin	–	Mouse mAb (clone 8d4, Sigma)
	Paxillin	–	Mouse mAb (Transduction Laboratory),
	P-Tyr	–	Mouse mAb (clone 9411, Cell Signaling, Beverly, MA)
Signaling proteins	RhoA	–	Mouse mAb (clone 26C4, Santa Cruz Biotech.)
	PKCε	–	Mouse mAb (clone E5, Santa Cruz Biotech.)
	MLCK	–	Mouse mAb (clone K-36, Sigma)
Cytoskeleton proteins	Vimentin	–	Mouse mAb (clone V9, Dako, Postfach, Switzerland).

mAb: monoclonal antibody; α-SMA: α-smooth muscle actin; P-Tyr: phosphorylated tyrosine; MHC: myosin heavy chain; MLC: myosin light chain; MLCK: myosin light chain kinase; PKC: protein kinase C.

biochemically. Western blot analyses with anti-GFP antibody showed a single 80 kDa band that corresponded to the predicted molecular mass of the α-SMA-EGFP protein [actin (42 kDa) + EGFP (36 kDa)] (Fig. 1C, lane 2). This band was also recognized by the anti-αsm-1 antibody, indicating that the antigenic properties of the Ac-EEED N-terminus were not altered by tagging the C-terminus with EGFP (Fig. 1C, lane 4). Both transfected and non-transfected cells showed the 42-kDa band of endogenous α-SMA (Fig. 1C, lanes 3 and 4).
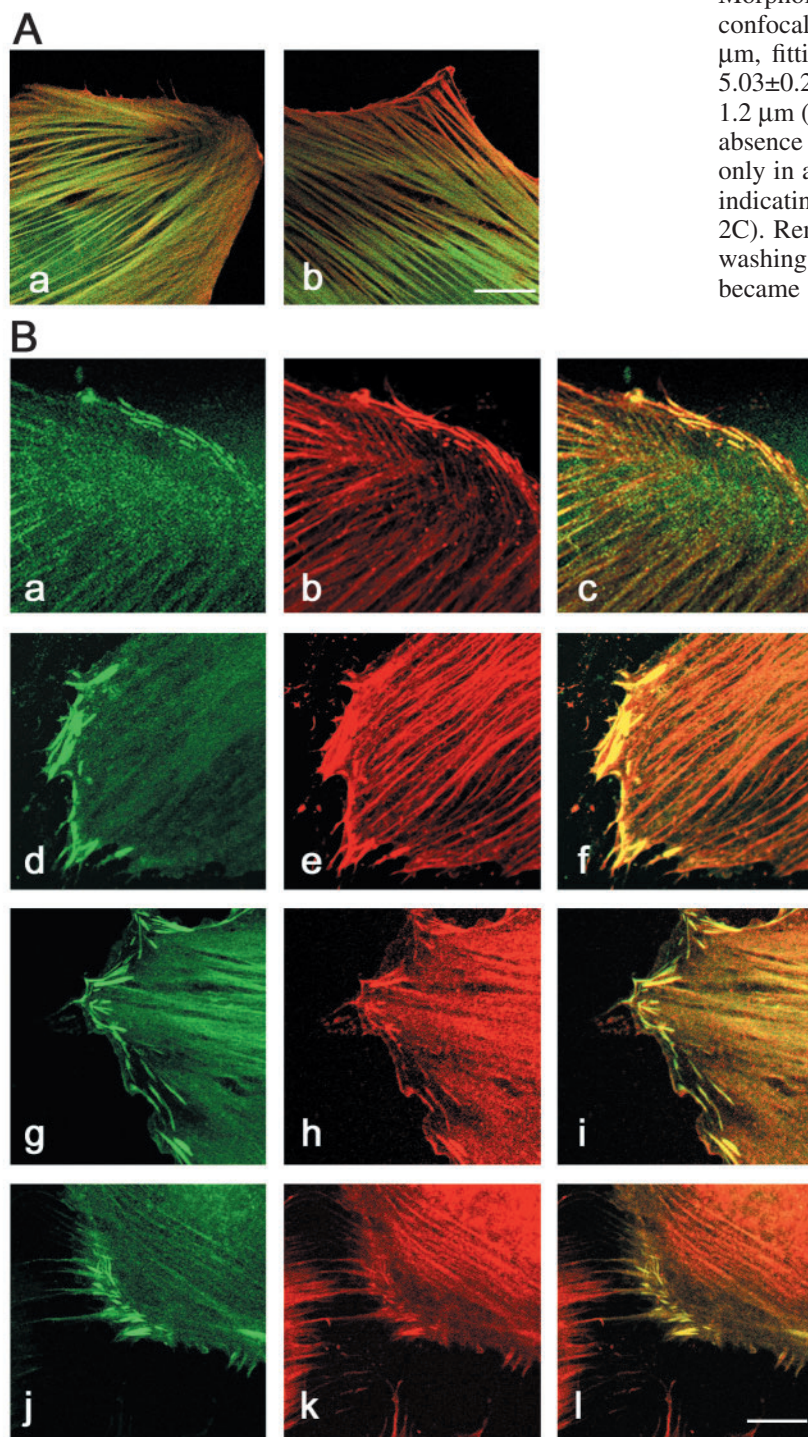
Time-lapse observation of α-SMA-EGFP in cells treated with SMA-FP

As a first step in understanding the function of Ac-EEED, we studied the effect of SMA-FP on the organization of α-SMA-EGFP in living cells. As shown in Fig. 2A, 5 μg/ml SMA-FP induced two phenomena visible 30 minutes after the beginning of the treatment: (1) the gradual decrease of fluorescence-intensity of α-SMA-EGFP in stress fibers and, (2) the time-correlated appearance of RLSs, mainly located at the cell periphery and close to stress fibers. Both effects were observed in approximately 60% of the transfected cells (Fig. 2C). Morphological features of RLSs were determined on digitized confocal images. The length of RLSs varied widely from 2-20 μm, fitting a Gaussian curve with a peak at 4 μm (average: 5.03±0.21, Fig. 2B). Their diameter ranged between 0.1 and 1.2 μm (average: 0.54±0.02). Controls, performed either in the absence of SMA-FP or the presence of SKA-FP, showed RLSs only in a minority of the cell population (7% at most), further indicating the specificity of the effect caused by SMA-FP (Fig. 2C). Removal of SMA-FP reversed its effects: after 1 hour of washing, RLSs completely disappeared and stress fibers became again highly fluorescent (Fig. 2C).

Interestingly, RLSs disappeared after permeabilizing cells with classic methods (such as 0.1% Triton-X100 for 1 minute following fixation with 1% paraformaldehyde); this susceptibility of RLSs to detergent may account for the fact that previously they have not been observed in non-transfected cells. We thus developed an alternative protocol for fixing cells, using 1% paraformaldehyde for 10 minutes followed by permeabilization with methanol (–20°C) for 3 minutes, allowing routine demonstration of these structures. Using this new method, we were able to obtain very clear antibody staining and RLS preservation and revealed that RLSs were also formed in 44.6±4.9% of non-transfected cells when treated with SMA-FP for 30 minutes (Fig. 2D), thus excluding the possibility of an artifact owing to EGFP. Similarly, SMA-FP provoked the formation of RLSs in myofibroblasts of various origins, such as rat lung fibroblasts and Dupuytren fibroblasts treated with TGFβ (data not shown).

Fig. 3. Presence of actin isoforms in the RLSs. (A) Overlay images of EGFP fluorescence (green) and (a) staining of β-cytoplasmic actin (red) or (b) γ-cytoplasmic actin (red) in non-treated α-SMA-EGFP-transfected cells are shown. Scale bar, 10 μm. (B) Cells were treated for 30 minutes with SMA-FP, fixed with 1% paraformaldehyde for 10 minutes followed by methanol incubation for 3 minutes and stained with either (b) anti β-cytoplasmic actin antibody, (e) γ-cytoplasmic actin antibody or (h) Alexa 568-phalloidin. (k) The distribution of rhodamine-labeled SMA-FP in α-SMA-EGFP-transfected cells was also investigated. α-SMA-EGFP patterns are shown in images a, d, g, and j and colocalization was visualized by confocal microscopy. Overlay images are shown in c, f, i and l. Bar, 10 μm.
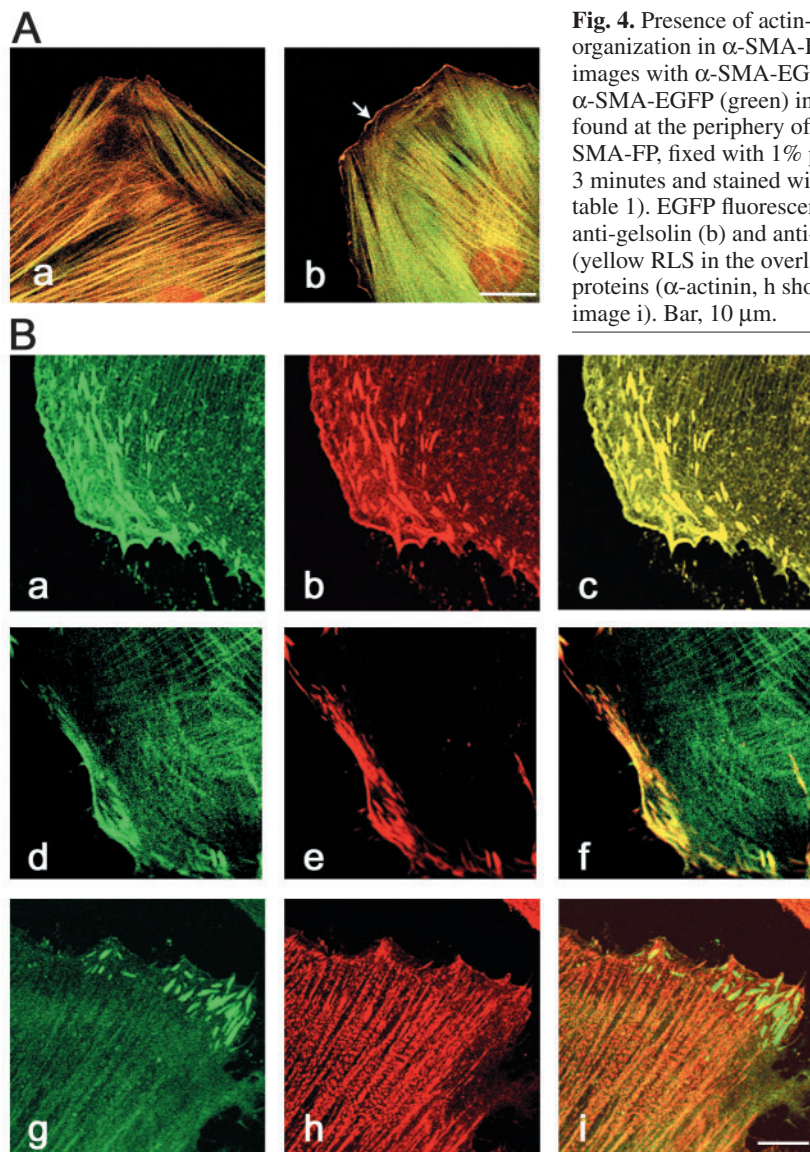
Fig. 4. Presence of actin-binding proteins in RLS. (A) Gelsolin (a) and cofilin (b) organization in α-SMA-EGFP transfected cells in control conditions. Overlay images with α-SMA-EGFP show that gelsolin (a, red) completely colocalized with α-SMA-EGFP (green) in stress fibers, whereas cofilin (b, red) was additionally found at the periphery of the cell (arrow). (B) Cells were treated for 30 minutes with SMA-FP, fixed with 1% paraformaldehyde for 10 minutes followed by methanol for 3 minutes and stained with a large panel of anti actin-binding protein antibodies (see table 1). EGFP fluorescence (green) and immunofluorescence staining (red) with anti-gelsolin (b) and anti-cofilin (e) showed that they were both present in RLS (yellow RLS in the overlay images c and f), whereas many other actin binding proteins (α-actinin, h shown as example) were not found (green RLS in the overlay image i). Bar, 10 μm.

arrow). Following SMA-FP treatment, gelsolin (Fig. 4B, a-c) and cofilin (Fig. 4B, d-f) were present in RLSs. No other actin-binding proteins examined (e.g. α-actinin, Fig. 4B, g-i, Table 1), were found in RLS (green RLSs in the overlay image i).

Spreading-experiments

To investigate whether RLSs occur during α-SMA re-organization in physiological conditions, we studied transfected REF-52 cells as they spread on planar culture surfaces, a process during which stress fibers are formed de novo. Four hours after seeding, α-SMA exhibited essentially three types of organization: (1) predominantly diffuse (not shown); (2) present in stress fibers (Fig. 5A, a) and, (3) arranged in RLSs, longitudinal to the cell membrane (Fig. 5A, b), showing the same molecular characteristics as described above (data not shown). The proportion of cells showing organization of α-SMA either in stress fibers or in RLSs varied, depending on how much time passed after seeding the cells (Fig. 5B). In particular, the percentage of cells displaying RLSs decreased from 37±3.7% at 4 hours after plating to 2.5±1.3% at 12 hours after plating. By contrast, a comparable increase in the number of cells displaying stress fibers was observed during the same interval. Continuous time-lapse observation of individual spreading cells (Fig. 5C) recurrently showed that RLSs first displayed a tangential orientation to the cell edge (t=0-3 hours), followed by reorientation perpendicularly to the cell edge (t=6-10 hours). Then, RLSs gradually became smaller and disappeared almost completely (t=12-15 hours) when α-SMA started to become organized in stress fibers. Importantly, during spreading, formation of α-SMA-positive stress fibers was severely impaired when, 2 hours after spreading, cells were treated with SMA-FP for 2 hours: 59.3±3.2% of the cells now contained tangential RLSs and only 5.1±1.0% of cells displayed α-SMA organized in stress fibers. This suggests that RLSs represent a step in the organization of α-SMA preceding their incorporation in stress fibers.

FRAP experiments

We used FRAP analysis of α-SMA-EGFP stress fibers to

Characterization of the RLSs

We determined the molecular composition of RLSs by immunostaining, to investigate which proteins might be associated with the RLSs and potentially interfere with the N-terminus of α-SMA. A large panel of primary antibodies was used in confocal microscopy, as listed in Table 1. All other actin isoforms expressed in REF-52 cells were partially present in RLSs, as demonstrated by the colocalization of EGFP with both β-cytoplasmic actin (Fig. 3B, a-c) and γ-cytoplasmic actin (Fig. 3B, d-f). The rhodamine-phalloidin staining of these structures (shown in Fig. 3B, g-i) indicated that they represent polymerized actin. In addition, after 30 minutes of treatment, SMA-FP was localized in all structures where α-SMA-EGFP was present (stress fibers as well as RLSs; Fig. 3B, j-l). Among all actin-binding proteins tested, only cofilin and gelsolin localized in RLSs together with α-SMA. In non-treated SM02 cells (Fig. 4A) and wild-type REF-52 cells (data not shown), gelsolin (Fig. 4A, a) and cofilin (Fig. 4A, b) both colocalized with α-SMA in stress fibers, appeared diffusely in the cytosol and, in the case of cofilin, in membrane ruffles (Fig. 4A, b,

determine whether SMA-FP interferes with α-SMA dynamics and incorporation into stress fibers. Photobleached regions appear as dark bars and squares (Fig. 6A,B); recovery of fluorescence was monitored at 1-minute intervals. In control conditions, fluorescence of bleached α-SMA-EGFP stress fibers (Fig. 6A) recovered almost completely within 30 minutes (see square), indicating a constant exchange between globular and polymerized α-SMA in living cells. Time-lapse observations also revealed that the bleached zones appearing as bars on individual stress fibers moved during fluorescence recovery at different rates and in opposite directions, resulting in a zig-zag pattern (Fig. 6, arrows). The average rate of movement of bleached zones was 2.4±0.2 µm/hour (*n*=51), regardless of the direction (Fig. 6C).

To follow the effects of SMA-FP on α-SMA-EGFP recovery in stress fibers, we purposely selected cells not displaying RLSs during the treatment but containing prominent and strongly fluorescent stress fibers. Fluorescence recovery in stress fibers was inhibited (Fig. 6B; see square) and rates of zig-zag movement were approximately fivefold slower than in non-treated cells, averaging 0.5±0.09 µm/hour (*n*=38) (Fig. 6C). To assess the rate of α-SMA-EGFP recovery in RLS, we bleached RLSs in cells treated with SMA-FP and quantified FRAP of α-SMA-EGFP. Thirty minutes after administration of SMA-FP, RLSs were bleached and FRAP was observed by live-cell imaging (Fig. 7A). FRAP started at the periphery of bleached RLSs within a few minutes after bleaching and occurred thereafter in the center of the structures but did not reach the fluorescence intensity of α-SMA-EGFP before bleaching. Quantification of FRAP (Fig. 7B) performed in the entire region bleached revealed that SMA-EGFP within RLSs recovers rapidly but only to half of the initial values (54.7±3.7%). Taken together, these data indicate that SMA-EGFP located at the border of RLSs exchanges more rapidly with the

α-SMA-EGFP pool in the cytoplasm, than α-SMA-EGFP in the center of the RLS.

Discussion

We have previously reported that in cultured myofibroblasts, delivery of the N-terminal Ac-EEED sequence of α-SMA fully abolishes staining for α-SMA (Chaponnier et al., 1995) and
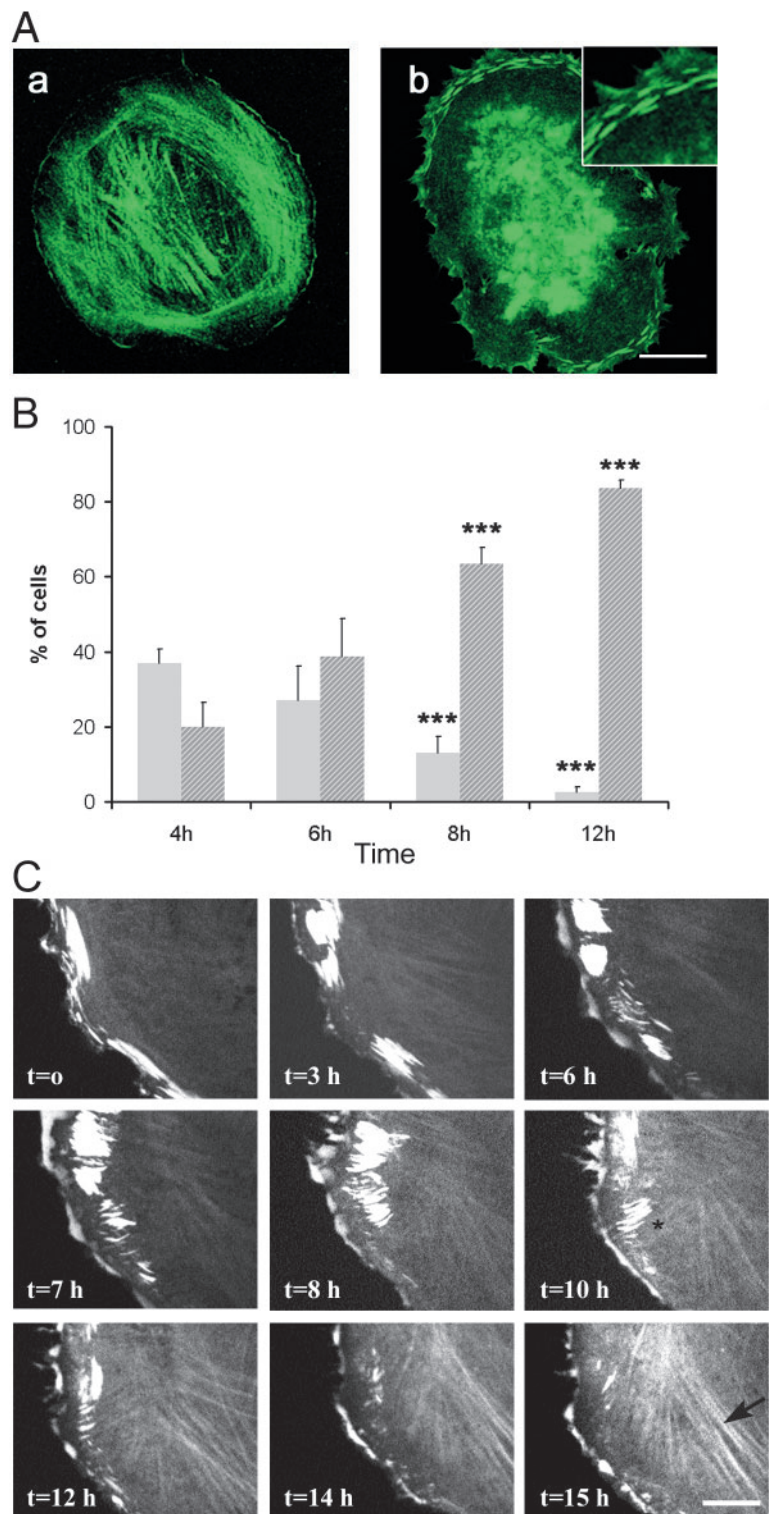

Fig. 5. Visualization of RLSs in spreading REF-52 cells transfected with α-SMA-EGFP. Cells were trypsinized, plated in F12 medium, allowed to spread and fixed at different time points with 1% paraformaldehyde for 10 minutes followed by methanol incubation for 3 minutes. (A) After 4 hours of spreading in the absence of SMA-FP, some cells exhibited α-SMA-positive stress fibers (a), whereas other cells (b) displayed RLSs that were arranged tangentially to the plasma membrane (see inset). Scale bar, 10 µm. (B) In a minimum of 200 cells, the percentage of cells displaying RLSs (gray bars) or stress fibers (hatched bars) was assessed at different time points after plating (4, 6, 8, and 8 hours). Bars represent s.e.m. (***P≤0.001, the 4-hour time point was taken as the reference). (C) Cells were seeded in observation chambers in F12 medium supplemented with 2% FCS and allowed to spread for 2 hours. Cell-spreading was recorded using a laser confocal spinning wheel (Nipkow disc) and images were acquired every 10 minutes for 15 hours. Scale bar, 20 µm. During spreading, cells first displayed RLSs that appeared perpendicular to the cell edge (*) and then gradually disappeared while α-SMA was organized in stress fibers (arrow).
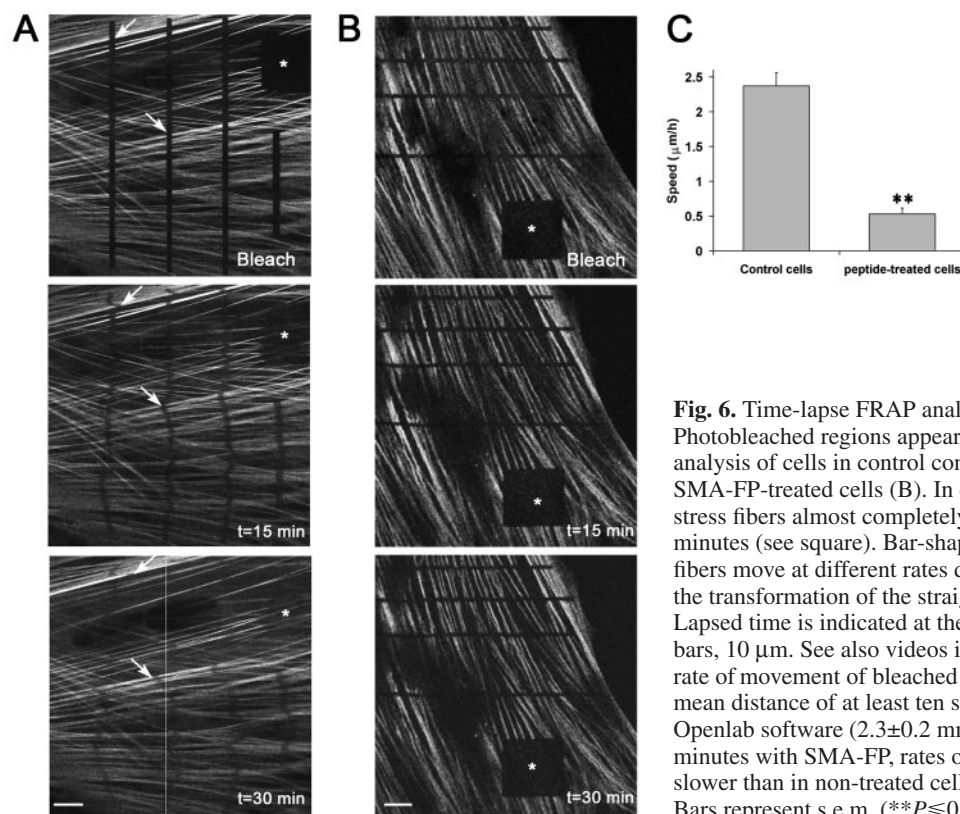
Fig. 6. Time-lapse FRAP analysis of α-SMA-EGFP stress fibers. Photobleached regions appear as dark bars and squares (*). FRAP analysis of cells in control conditions (A) was compared with that of SMA-FP-treated cells (B). In control conditions, bleached α-SMA-EGFP stress fibers almost completely recovered their fluorescence within 30 minutes (see square). Bar-shaped bleached zones on individual stress fibers move at different rates during fluorescence recovery, as indicated by the transformation of the straight bleach zone into a zig-zag line (arrows). Lapsed time is indicated at the lower right corner of each image. Scale bars, 10 µm. See also videos in supplementary material. (C) The average rate of movement of bleached zones was quantified by measuring the mean distance of at least ten stress fibers in at least ten cells using Openlab software (2.3±0.2 mm/hour (n=51). In cells pre-treated for 15 minutes with SMA-FP, rates of movement were approximately fivefold slower than in non-treated cells, averaging 0.53±0.09 µm/hour (n=38). Bars represent s.e.m. (**$P \leq 0.001$ compared with control cells).

inhibits contractile activity (Hinz et al., 2002), demonstrating that this sequence has a major and specific effect on α-SMA organization and function. As a first step towards the understanding of the mechanisms involved, we have now visualized the effect of SMA-FP on α-SMA incorporation into stress fibers of living cells, using EGFP-tagged α-SMA.

Because the N-terminus determines the specificity of actin isoforms and, in the case of α-SMA, is crucial for the effect of SMA-FP on α-SMA polymerization (Chaponnier et al., 1995) and myofibroblast contraction (Hinz et al., 2002), we thought it important to fuse EGFP at the C-terminus. However, previous studies with a *Drosophila melanogaster*-specific actin isoform (Brault et al., 1999) have shown that the C-terminus of actin is more sensitive to tagging than is the N-terminus. Therefore, we included a spacer (11 amino acid VSV-G epitope tag) (von Arx et al., 1995) between actin and EGFP, to avoid that EGFP interferes with the correct folding of the protein. Using this strategy, we generated cell clones expressing α-SMA-EGFP that, by the standards we used, behave similar to the endogenous protein, namely its intracellular organization in response to serum concentration and TGFβ treatment.

The concomitant disappearance of α-SMA from stress fibers and the appearance of RLSs following SMA-FP treatment might be because of (i) the dissociation of α-SMA from pre-existing stress fibers and its recruitment to these new structures or (ii) blocked incorporation of α-SMA into stress fibers by SMA-FP and its subsequent accumulation in RLSs, which might represent an intermediate step in stress fiber organization. Although we cannot completely exclude the first possibility, the data presented here strongly suggest that SMA-FP blocks stress fiber formation of α-SMA: (1) RLSs also appear in non-transfected myofibroblasts in normal culture conditions, albeit more sporadically than after treatment with SMA-FP, which argues for the transient state of RLS. (2) During normal myofibroblast spreading, when stress fibers are de novo formed from a large pool of disassembled actin, RLSs are particularly prominent before the formation of stress fibers. (3) During cell spreading and in the presence of SMA-FP, cells are unable to form stress fibers and any organization of α-SMA appears to be arrested at the level of RLSs. (4) In non-treated cells, SMA-FP significantly diminishes the rate of zig-zag movements characteristic of fluorescence-recovery in the bar-shaped appearances of bleached regions in stress fibers, as shown in our FRAP experiments. We have previously shown that SMA-FP has a potent effect on cell contraction (Hinz et al., 2002). This raises the question whether the decrease of zig-zag movement observed in the FRAP experiments is a consequence of inhibited cell contraction or whether the diminution of α-SMA reassembly into stress fibers is the initial phenomenon, occurring after SMA-FP treatment. It is difficult to rule out the first possibility. We favor, however, the possibility that incorporation of α-SMA into stress fibers is inhibited because no recovery occurs in square-shaped bleached zones of cells treated with SMA-FP. In addition α-SMA-EGFP was incorporated uniformly along stress fibers in non-treated cells, as previously shown with microinjected fluorescent actin (Turnacioglu et al, 1998). A consequence of this inhibition would be a reduced α-SMA-dependent contractile activity (Hinz et al., 2002). Thus, experiments with SMA-FP have allowed us to hypothesize a new mechanism of stress-fiber-formation as illustrated in Fig. 8. Several interesting aspects of actin assembly have emerged from this

study. The RLS represents a hitherto unknown structure, which appears to function as a reservoir for pre-polymerized α-SMA during stress-fiber-formation. Its visualization was facilitated by blocking incorporation of α-SMA into stress fibers by SMA-FP. However, RLSs may also be interpreted as a stress-related response, where they would then represent a temporary rescue mechanism for the cell. Although both explanations are not mutually exclusive, the disappearance of RLSs in favor of stress-fiber-formation during normal cell spreading suggests that, in one given population, all cells that form stress fibers will experience this phase. This strongly argues that RLSs are an intermediate α-SMA-organization preceding stress fiber formation, rather than being part of an erroneous, occasionally occurring pathway.

Fig. 7. FRAP analysis of SMA-EGFP turnover in RLSs. (A) Transfected cells were treated for 30 minutes with SMA-FP. α-SMA-EGFP RLSs were photobleached and images were taken at indicated time points. Bar, 5 μm. (B) Fluorescence intensities were measured at different times using Openlab software and related to the intensity measured in the first video frame. Fluorescence before bleaching was normalized to 100%. Each data point represents the mean intensity of fluorescence of 33 RLSs analyzed in eight different cells. Bars represent s.e.m.

The fact that RLSs are lost when using classic cell-permeabilization procedures with detergent, might explain why they have not been described previously. The effect of detergents and the sub-cellular localization of RLSs, suggest that RLSs are somehow connected with the plasma membrane. This is in agreement with the notion that actin polymerization is initiated at the plasma membrane through phosphatidylinositol (4,5)-bisphosphate (for a review, see Yin and Janmey, 2003). Additional important clues regarding the origin of RLSs are provided by their molecular composition. None of the architectural stress fiber proteins (e.g. α-actinin, myosin-heavy chain, tropomyosin) became dissociated from stress fibers following treatment with SMA-FP. Despite the resemblance of RLSs to focal adhesions in some cells, none of the focal adhesion proteins we examined were found in RLSs. It has recently been postulated that thrombin activation leads to the formation of a protein kinase Cε (PKCε)-RhoA-αSMA ternary complex, leading to stress fiber formation of α-SMA (Bogatkevich et al., 2003). Neither PKCε nor Rho-A, however, were found in RLS. In fact, of the tested actin-binding proteins, only cofilin and gelsolin were present in RLSs. Gelsolin

belongs to a family of proteins that are essential for microfilament remodeling (Burtnick et al., 1997; Kwiatkowski et al., 1986; Yin, 1987). In vitro, gelsolin interacts with G-actin and F-actin, promotes nucleation and both severs and caps actin filaments. Cofilin belongs to another family of actin-binding proteins also severing actin filaments, therefore increasing polymerization dynamics (Bamburg, 1999). The presence of these two proteins is consistent with the hypothesis that SMA-FP interferes with actin-dynamics. In addition, although both cytoplasmic actins do not disappear from stress fibers as previously observed (Hinz et al, 2002), a small proportion of them accompanied α-SMA in RLSs.

In conclusion, we propose a model that identifies the importance of the N-terminal AcEEED sequence for α-SMA organization and function. We suggest that RLSs represent an intermediate step in the process of α-SMA incorporation into stress fibers and possibly provide an α-SMA reservoir when this incorporation process is disturbed. The presence of gelsolin and cofilin in RLS suggests their active participation in this process. Because SMA-FP blocks α-SMA at this step, we propose that the peptide interferes with a putative partner
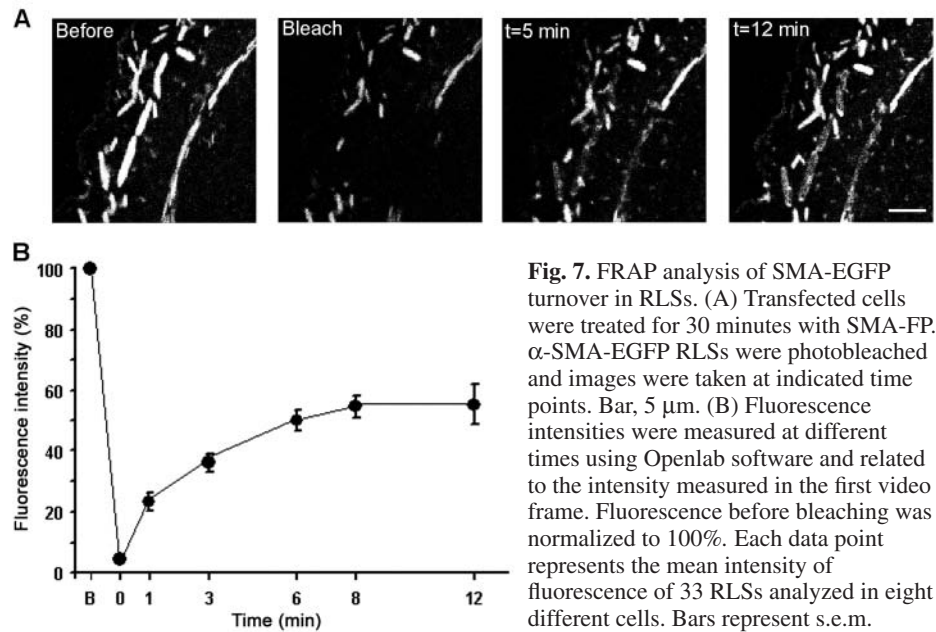
Fig. 8. Schematic representation of the proposed mechanism of SMA-FP action and stress-fiber-formation. (a) α-SMA incorporation in pre-existing cytoplasmic-actin-containing stress fibers represented as light red dashed lines. α-SMA is first recruited in RLSs, a pre-requisite step before its incorporation in stress fibers (see arrows). (b) α-SMA incorporation into stress fibers (dark red lines) confers higher cell-contractility (illustrated by the arrows on the top of the cell). When such contractile

cells are treated with SMA-FP, α-SMA incorporation in stress fibers is inhibited (see zoomed-in part of the cell c), resulting in α-SMA accumulation in RLSs, its disappearance from stress fibers, and subsequently 'relaxation' of the cell.
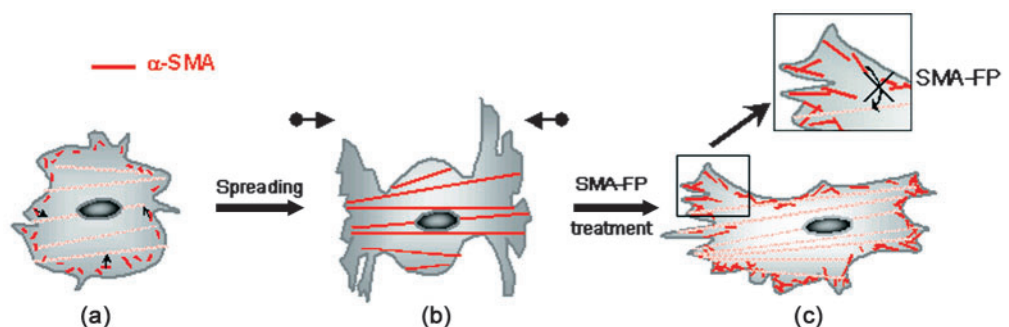
of α-SMA allowing its incorporation in stress fibers. Whether this process is limited to incorporation of α-SMA or it is a general phenomenon that occurs with all actin isoforms remains to be determined.

References

Bamburg, J. R. (1999). Proteins of the ADF/cofilin family: essential regulators of actin dynamics. *Annu. Rev. Cell. Dev. Biol.* **15**, 185-230.
Benzonana, G., Skalli, O. and Gabbiani, G. (1988). Correlation between the distribution of smooth muscle or non muscle myosins and alpha-smooth muscle actin in normal and pathological soft tissues. *Cell. Motil. Cytoskeleton* **11**, 260-274.
Bogatkevich, G. S., Tourkina, E., Abrams, C. S., Harley, R. A., Silver, R. M. and Ludwicka-Bradley, A. (2003). Contractile activity and smooth muscle alpha-actin organization in thrombin-induced human lung myofibroblasts. *Am. J. Physiol. Lung Cell Mol. Physiol.* **285**, L334-343.
Brault, V., Sauder, U., Reedy, M. C., Aebi, U. and Schoenenberger, C. A. (1999). Differential epitope tagging of actin in transformed Drosophila produces distinct effects on myofibril assembly and function of the indirect flight muscle. *Mol. Biol. Cell* **10**, 135-149.
Burtnick, L. D., Koepf, E. K., Grimes, J., Jones, E. Y., Stuart, D. J., McLaughlin, P. J. and Robinson, R. C. (1997). The crystal structure of plasma gelsolin: implications for actin severing, capping, and nucleation. *Cell* **90**, 661-670.
Chaponnier, C. and Gabbiani, G. (1989). Gelsolin modulation in epithelial and stromal cells of mammary carcinoma. *Am. J. Path.* **134**, 597-603.
Chaponnier, C., Goethals, M., Janmey, P. A., Gabbiani, F., Gabbiani, G. and Vandekerckhove, J. (1995). The specific NH2-terminal sequence Ac-EEED of alpha-smooth muscle actin plays a role in polymerization in vitro and in vivo. *J. Cell Biol.* **130**, 887-895.
Darby, I., Skalli, O. and Gabbiani, G. (1990). α-smooth muscle actin is transiently expressed by myofibroblasts during experimental wound healing. *Lab. Invest.* **63**, 21-29.
Derossi, D., Joliot, A. H., Chassaing, G. and Prochiantz, A. (1994). The third helix of the Antennapedia homeodomain translocates through biological membranes. *J. Biol. Chem.* **269**, 10444-10450.
Herman, I. M. (1993). Actin isoforms. *Curr. Opin. Cell Biol.* **5**, 48-55.
Hinz, B., Gabbiani, G. and Chaponnier, C. (2002). The NH2-terminal peptide of α-smooth muscle actin inhibits force generation by the myofibroblast in vitro and in vivo. *J. Cell Biol.* **157**, 657-663.
Hinz, B., Dugina, V., Ballestrem, C., Wehrle-Haller, B. and Chaponnier, C. (2003). Alpha-smooth muscle actin is crucial for focal adhesion maturation in myofibroblasts. *Mol. Biol. Cell* **14**, 2508-2519.
Khaitlina, S. Y. (2001). Functional specificity of actin isoforms. *Int. Rev. Cytol.* **202**, 35-98.
Kreis, T. E., Winterhalter, K. H. and Birchmeier, W. (1979). In vivo distribution and turnover of fluorescently labeled actin microinjected into human fibroblasts. *Proc. Natl. Acad. Sci. USA* **76**, 3814-3818.

Kwiatkowski, D. J., Stossel, T. P., Orkin, S. H., Mole, J. E., Colten, H. R. and Yin, H. L. (1986). Plasma and cytoplasmic gelsolins are encoded by a single gene and contain a duplicated actin-binding domain. *Nature* **323**, 455-458.
Laemmli, U. K. (1970). Cleavage of structural proteins during the assembly of the head of bacteriophage T4. *Nature* **227**, 680-685.
Lennette, D. A. (1978). An improved mounting medium for immunofluorescence microscopy [letter]. *Am. J. Clin. Pathol.* **69**, 647-648.
Mounier, N., Perriard, J.-C., Gabbiani, G. and Chaponnier, C. (1997). Transfected muscle and non-muscle actins are differentially sorted by cultured smooth muscle and non-muscle cells. *J. Cell Sci.* **110**, 839-846.
Moustakas, A. and Stournaras, C. (1999). Regulation of actin organisation by TGF-beta in H-ras-transformed fibroblasts. *J. Cell Sci.* **112**, 1169-1179.
Percival, J. M., Thomas, G., Cock, T. A., Gardiner, E. M., Jeffrey, P. L., Lin, J. J., Weinberger, R. P. and Gunning, P. (2000). Sorting of tropomyosin isoforms in synchronised NIH 3T3 fibroblasts: evidence for distinct microfilament populations. *Cell Motil. Cytoskeleton* **47**, 189-208.
Pfitzer, G., Sonntag-Bensch, D. and Brkic-Koric, D. (2001). Thiophosphorylation-induced Ca(2+) sensitization of guinea-pig ileum contractility is not mediated by Rho-associated kinase. *J. Physiol.* **533**, 651-664.
Powell, D. W., Mifflin, R. C., Valentich, J. D., Crowe, S. E., Saada, J. I. and West, A. B. (1999). Myofibroblasts. I. Paracrine cells important in health and disease. *Am. J. Physiol.* **277**, C1-9.
Rodal, A. A., Tetreault, J. W., Lappalainen, P., Drubin, D. G. and Amberg, D. C. (1999). Aip1p interacts with cofilin to disassemble actin filaments. *J. Cell. Biol.* **145**, 1251-1264.
Rubenstein, P. A. (1990). The functional importance of multiple actin isoforms. *BioEssays* **12**, 309-315.
Sappino, A. P., Schürch, W. and Gabbiani, G. (1990). Differentiation repertoire of fibroblastic cells: expression of cytoskeletal proteins as markers of phenotypic modulations. *Lab. Invest.* **63**, 144-161.
Schmitt-Graff, A., Desmouliere, A. and Gabbiani, G. (1994). Heterogeneity of myofibroblast phenotypic features: an example of fibroblastic cell plasticity. *Virchows Arch.* **425**, 3-24.
Serini, G. and Gabbiani, G. (1999). Mechanisms of myofibroblast activity and phenotypic modulation. *Exp. Cell Res.* **250**, 273-283.
Skalli, O., Ropraz, P., Trzeciak, A., Benzonana, G., Gillessen, D. and Gabbiani, G. (1986). A monoclonal antibody against α-smooth muscle actin: a new probe for smooth muscle differentiation. *J. Cell Biol.* **103**, 2787-2796.
Svitkina, T. M., Bulanova, E. A., Chaga, O. Y., Vignjevic, D. M., Kojima, S., Vasiliev, J. M. and Borisy, G. G. (2003). Mechanism of filopodia initiation by reorganization of a dendritic network. *J. Cell Biol.* **160**, 409-421.
Tomasek, J. J., Gabbiani, G., Hinz, B., Chaponnier, C. and Brown, R. A. (2002). Myofibroblasts and mechano-regulation of connective tissue remodelling. *Nat. Rev. Mol. Cell Biol.* **3**, 349-363.
Towbin, H., Staehelin, T. and Gordon, J. (1979). Electrophoretic transfer of proteins from polyacrylamide gels to nitrocellulose sheets: procedure and some applications. *Proc. Natl. Acad. Sci. USA* **76**, 4350-4354.
Turnacioglu, K. K., Sanger, J. W. and Sanger, J. M. (1998). Sites of monomeric actin incorporation in living PTK2 and REF-52 cells. *Cell Motil. Cytoskel.* **40**, 59-70.
Vandekerckhove, J. and Weber, K. (1978). Actin amino-acid sequences. Comparison of actins from calf thymus, bovine brain, and SV40-transformed mouse 3T3 cells with rabbit skeletal actin. *Eur. J. Biochem.* **90**, 451-462.
von Arx, P., Bantle, S., Soldati, T. and Perriard, J. C. (1995). Dominant negative effect of cytoplasmic actin isoproteins on cardiomyocyte cytoarchitecture and function. *J. Cell Biol.* **131**, 1759-1773.
Yin, H. L. (1987). Gelsolin: calcium- and polyphosphoinositide-regulated actin-modulating protein. *BioEssays* **7**, 176-179.
Yin, H. L. and Janmey, P. A. (2003). Phosphoinositide regulation of the actin cytoskeleton. *Annu. Rev. Physiol.* **65**, 761-789.